ELSEVIER

Ceramics International 28 (2002) 387–392

CERAMICS INTERNATIONAL

www.elsevier.com/locate/ceramint

# The effects of carbon addition on the mechanical properties of $MoSi_2$–TiC composites

Zeng Yuping*, Chao-Nan Xu, T. Watanabe

*Department of Inorganic Composites Materials, Kyushu National Industrial Research Institute, Saga 841-0052, Japan*

Received 25 February 2001; received in revised form 10 July 2001; accepted 3 August 2001

**Abstract**

In order to improve the mechanical properties of $MoSi_2$ matrix composites, carbon was added to a $MoSi_2$–20 wt.% TiC composite to remove the oxygen which exists at the grain boundaries as glassy $SiO_2$ phase. Compared with the $MoSi_2$–20 wt.% TiC composite without carbon addition, the bending strength and fracture toughness of a $MoSi_2$–20 wt.% TiC–1 wt.% C composite sintered at 1600 °C can be enhanced from 481 to 689 MPa and from 3.89 to 5.4 MPa·$m^{1/2}$ respectively. The experimental results show that the sintering temperature has a considerable effect on the mechanical properties of $MoSi_2$–20 wt.% TiC–1 wt.% C composites. As a deoxidant, carbon can react with glassy $SiO_2$ to eliminate the glassy $SiO_2$ phase. However, a further increase of carbon addition, beyond 1 wt.% produces an abatement of the mechanical properties. 

*Keywords:* A. Hot-pressing; A. Sintering; C. Mechanical properties; Molybdenum disilicide

## 1. Introduction

Molybdenum disilicide ($MoSi_2$) is an attractive high temperature structural material due to its high melting point and excellent oxidation resistance at high temperature. However, the mechanical properties of $MoSi_2$ have severely limited its application as a structural material. Many efforts have been made to strengthen $MoSi_2$ matrix composites by adding second phase particles, whiskers or fibers [1–7]. Due to preparation methods such as fusing or crushing, $MoSi_2$ powder always contains a large amount of oxygen. Therefore, the monolithic $MoSi_2$ always contains a glassy phase, which is one of the main factors that influence the mechanical properties of the materials not only at room temperature but also at high temperature. In order to eliminate the negative effects of the glassy $SiO_2$ phase, several methods have been introduced, such as HF washing, carbothermal or hydrogen reduction, aluminum addition, and in-situ formation of the more stable double oxide [8–11]. TiC is another potential reinforcement for $MoSi_2$ with potential advantages: (1) TiC has a brittle-to-ductile transition above 600 °C, (2) the thermal expansion coefficient of TiC is nearly the same as that of $MoSi_2$, and (3) thermodynamic calculations indicate that TiC and $MoSi_2$ should not react at the temperatures used for densification of the $MoSi_2$ [12–14]. As a deoxidant, carbon has been used to remove oxygen in $MoSi_2$ [1]. Maloy et al. [15] have studied the effect of 2 wt.% carbon addition on the mechanical properties of $MoSi_2$, it was reported that carbon can react with the siliceous grain boundary phase to form SiC and $Mo_{\leqslant 5}Si_3C_{\leqslant 1}$, thereby increasing the high temperature fracture toughness and bending strength considerably. Maxwell [16] has reported that carbon addition increased the bending strength of hot-pressed $MoSi_2$ samples by 50% at 1100 °C. According to Pho et al. [17], the room temperature hardness and the indentation toughness of $MoSi_2$–20 vol.% TiC composites were greatly increased by TiC addition (from 2.11 to 9.82 MPa $m^{1/2}$). The objective of this study is to investigate the effect of carbon addition on the mechanical properties of $MoSi_2$–20 wt.% TiC.

## 2. Experimental procedure

The starting $MoSi_2$ powder (6 μm, Japan New Metals), after 72-h ball milling in ethanol, washing by

* Corresponding author. Present address: Max-Planck Institute for Metal Research, Powder Metallurgy Laboratory, Heisenberg Street. 5, D-70569 Stuttgart, Germany. Tel.: +49-711-6893-235; fax: +49-711-6893-131.

*E-mail address:* zeng@mf.mpg.de (Z. Yuping).

0272-8842/02/$22.00 
PII: S0272-8842(01)00106-7

HCl and drying, was used in the experiment. TiC powder (1.1 μm, Japan New Metals) and carbon powder (3 μm, Japan Carbon) were also used. These powders were mixed by dry ball-milling for 24 h, then the mixed powder was packed in graphite dies and hot-pressing was performed at different temperatures under 25 MPa in a vacuum for 1 h. The sintered disks were cut into test rods. Rectangular beam samples 2×4×12 mm were used to measure the three-point bending strength with a span of 10 mm at a crosshead speed of 0.5 mm/min; mirror-polished samples were used to test the indentation fracture toughness and hardness, using a load of 20 kg and an indentation time of 15 s for the measurement. Hardness ($H_v$) was evaluated by Vickers indentation. Fracture toughness ($K_{IC}$) at room temperature was determined simultaneously by the indentation fracture method. The value of $K_{IC}$ was calculated according to the equation [18]:

$$K_{IC} = 0.203(c/a)^{-3/2} H_v a^{1/2} \quad (1)$$

where $c$ and $a$ are the lengths of a median crack and half of a diagonal of an indentation, respectively. Phase analysis was conducted by X-ray diffraction (XRD). Microstructure characterization of the hot-pressed samples was performed using scanning electron microscopy (SEM). An energy-dispersive X-ray spectrometer (EDS) was used to determine the composition of the composite. The density of the samples was determined by Archimedes' principle using distilled water.

## 3. Results and discussion

### 3.1. Phase analysis and microstructure of the composites

Fig. 1 shows the XRD patterns for the monolithic $MoSi_2$ and $MoSi_2$–20 wt.% TiC composite with and without carbon addition. The XRD analysis indicates that the monolithic $MoSi_2$ sample contains $MoSi_2$ and $SiO_2$ (cristobalite PDF-27-0605). Perhaps, a small amount of amorphous $SiO_2$ crystallized and transformed into cristobalite during hot-pressing. Except for $MoSi_2$ (PDF 41-0612) and cubic TiC (PDF 71-0298), the $SiO_2$ peak can also be found in the $MoSi_2$–20 wt.% TiC composite, but the intensity of the $SiO_2$ peak in $MoSi_2$–20 wt.% TiC is smaller than that in the monolithic $MoSi_2$. By addition of 1 wt.% carbon to the $MoSi_2$–20 wt.%TiC composite, the $SiO_2$ peaks have completely disappeared. The XRD patterns of the $MoSi_2$–20 wt.% TiC–5 wt.% C composite sintered at 1700°C are different, and SiC peaks can be observed.

Fig. 2 shows SEM micrographs of composites sintered at 1600 °C with different carbon contents: (a) monolithic $MoSi_2$; (b) $MoSi_2$–20 wt.% TiC; (c) $MoSi_2$–20 wt.% TiC–1 wt.% C; (d) $MoSi_2$–20 wt.% TiC–5 wt.% C; (e) $MoSi_2$–20 wt.% TiC–10 wt.% C; and (f) $MoSi_2$–20 wt.% TiC–1 wt.% C (1700 °C). The microstructures of all the composites mainly consist of two phases, a matrix phase and a reinforcement phase. In Fig. 2a the grey area is the $MoSi_2$ phase and the black area is the $SiO_2$ phase. The glassy $SiO_2$ on the surface of $MoSi_2$ particles is mainly concentrated at the triple points during sintering, and the SEM micrograph shows the black $SiO_2$ points on the polished sample surface. After adding TiC powder to the $MoSi_2$ matrix, the microstructure of the $MoSi_2$–20 wt.% TiC is different from the monolithic $MoSi_2$, the grey phase is still the $MoSi_2$ matrix, the dark-grey phase is TiC. However, the glassy $SiO_2$ merged into the TiC phase so that the evident black $SiO_2$ points have disappeared. The microstructures of Figs. 2b–d are different from Fig. 2e. When the content of carbon addition reaches 5 wt.%, there is excess carbon in the composite, and many holes can be seen in the polished surface of the composites, because the hardness of carbon is not high, and it can be easily removed by polishing.

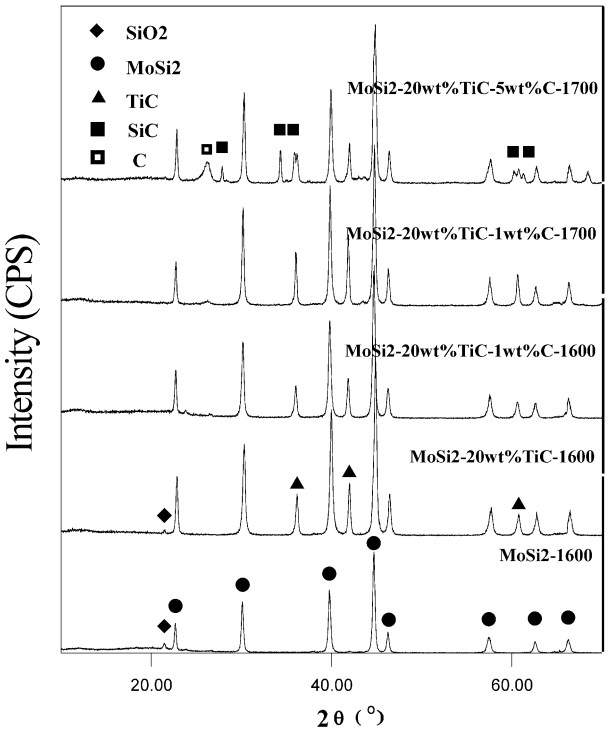


Fig. 1. XRD patterns for monolithic pure $MoSi_2$, $MoSi_2$–20 wt.% TiC composite with and without carbon addition.

Fig. 3 shows the EDX analyses patterns of Fig. 2b. The results show that the grey phase is the $MoSi_2$ matrix and the dark gray phase is TiC, and there is no evident oxygen signal in either of the particles. It is clear from SEM micrograph Fig. 2b that apart from the grey phase $MoSi_2$ matrix and the dark-grey TiC reinforced particle in the $MoSi_2$–20 wt.% TiC composites, there are still many black points distributed in the $MoSi_2$ matrix. EDX analysis reveals that the black particles consist of Si, Mo, Ti, O, and C. However, the $MoSi_2$–20 wt.% TiC

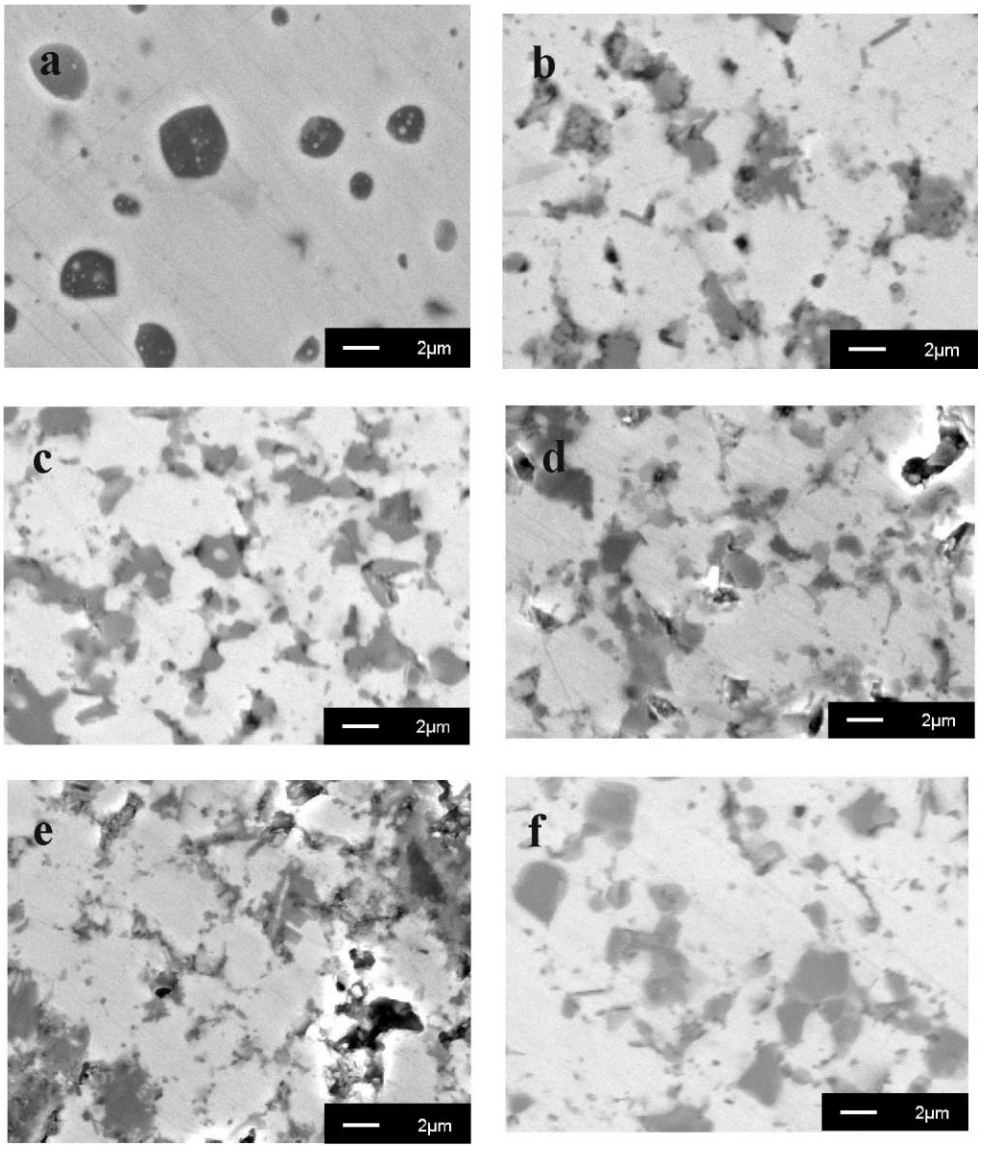


Fig. 2. SEM micrographs of polished composite surfaces (1600 °C).

composites with carbon addition do not have the black particles. Compared with the monolithic $MoSi_2$ Fig. 2a, the content of oxygen significantly decrease due to the TiC addition. With the carbon addition, the content of oxygen decreases in advance, and the oxygen signal has disappeared with 1 wt.% carbon addition. The results show that carbon is useful in removing oxygen from the $MoSi_2$ matrix composites due to chemical reactions.

Oxygen, which exists on the surface of the $MoSi_2$ particles as a glassy $SiO_2$ phase, is harmful to the mechanical properties of $MoSi_2$ matrix composite. Normally, the glassy $SiO_2$ mainly accumulates at triple points after sintering. There are many methods to eliminate the negative effects, adding a reducing agent is one of the methods. When the reducing agent carbon is added to $MoSi_2$, some chemical reactions will occur between the matrix and the additives during hot-pressing sintering [15].

$$SiO_2 + C \rightarrow SiC + CO + CO_2 \quad (2)$$

$$5MoSi_2 + 8C \rightarrow Mo_5Si_3C + 7SiC \quad (3)$$

$$MoSi_2 + 3SiO_2 + 2C \rightarrow 2SiC + MoO_3\,(g) + 3SiO\,(g) \quad (4)$$

Maloy et al. [15] found that a 2 wt.% carbon addition to $MoSi_2$ can form SiC and $Mo_5Si_3C$ (Nowotny phase) due to the reaction of carbon with glassy $SiO_2$ and $MoSi_2$. However, in this experiment, the $Mo_5Si_3C$ peaks cannot be found in all XRD patterns. The microstructures of all the composites consist of two kinds of particles. This is because the glassy $SiO_2$ phase is easily fused with TiC during sintering and reacts with the well-dispersed impurity carbon produced by the preparation process of the TiC powder . It can be explained that the intensity

of $SiO_2$ in $MoSi_2$–20 wt.% TiC is lower than that in the monolithic $MoSi_2$, but the content of carbon in TiC powder is not enough to eliminate the glassy $SiO_2$ completely. Therefore, an oxygen signal appeared in the EDX pattern of Fig. 3. Perhaps, the content of SiC in $MoSi_2$–20 wt.% TiC–1 wt.% C is small or SiC exists as an amorphous phase in the composites sintered at 1600 °C. The SiC peaks cannot be detected, even though the $MoSi_2$–20 wt.% TiC–1 wt.% C composites are sintered at 1700°C. However, SiC peaks can be found in $MoSi_2$–20 wt.% TiC–5 wt.% C composite sintered at 1700 °C, as the residual carbon reacts with $MoSi_2$ and forms a considerable amount of SiC in accord with Eq. (4).

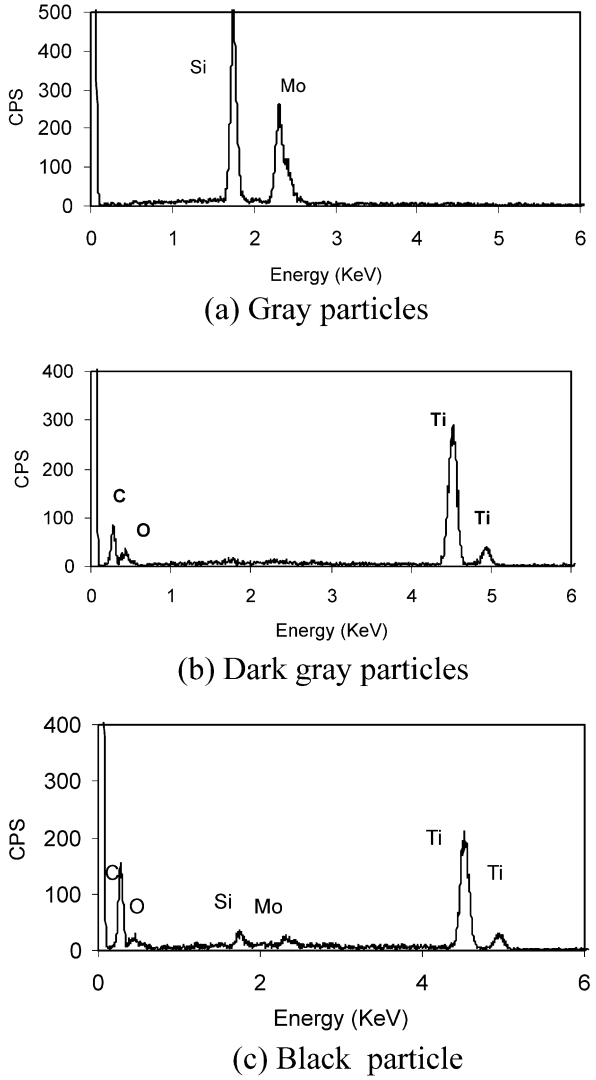


Fig. 3. EDX analyses patterns of Fig. 2b.

### 3.2. Mechanical properties

#### 3.2.1. Carbon content effect on the mechanical properties of $MoSi_2$–TiC composites

To investigate the effect of carbon addition on the mechanical properties, a $MoSi_2$–20 wt.% TiC composite was selected. Fig. 4 shows the effect of carbon content on the bending strength and fracture toughness of the composite. The bending strength of $MoSi_2$–20 wt.% TiC without carbon addition is about 481 MPa. With an increase of carbon content, the bending strength of $MoSi_2$–20 wt.% TiC composite sintered at 1600 °C increases, then decreases. The maximum bending strength is reached for a content of C of 1 wt.% and amounts to about 689 MPa. However, the bending strength of a composite with 10 wt.% C is only 265 MPa, which is lower than that of the monolithic $MoSi_2$. The corresponding toughness of $MoSi_2$–20 wt.% TiC–1 wt.% C composite sintered at 1600 °C is about 5.4 MPa $m^{1/2}$, which is higher than that of the monolithic $MoSi_2$ sample, amounting to 2.56 MPa $m^{1/2}$. The improvement of the mechanical properties can be explained by a reaction of carbon with the glassy $SiO_2$, which dislocates the continuous glass phase in MoSi–20 wt.% TiC composite grain boundaries. However, when the carbon content is much more than the necessary to remove the glassy $SiO_2$, the remnant carbon at the grain boundaries introduces flaws in the composites, because it is very difficult for carbon to densify at the sintering temperature and pressure. SEM micrographs in Fig. 2d and e also show evidence of such flaws.

Vicker Hardness ($H_v$) of $MoSi_2$–20 wt.% TiC composites decreases with increasing carbon content as shown in Fig. 5. $H_V$ changes from 14.8 GPa for $MoSi_2$–20 wt.% TiC to 6.95 GPa for $MoSi_2$–20 wt.% TiC–10 wt.% C. Although carbon addition can remove the glassy $SiO_2$ boundary phase with an improvement of strength and toughness of the composite, it reduces the density of the

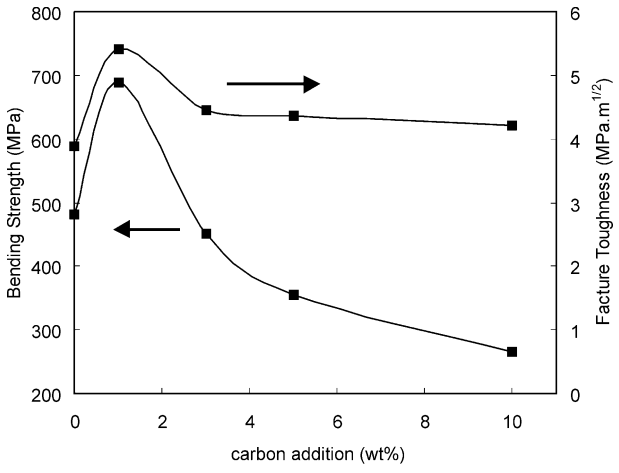


Fig. 4. Effect of carbon content on the bending strength and fracture toughness of the $MoSi_2$–20 wt.% TiC composites.

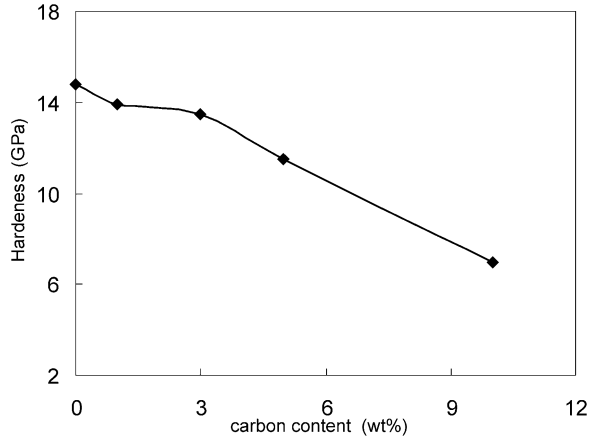


Fig. 5. Relation of Vicker hardness of $MoSi_2$–20 wt.% TiC composites with carbon as additive ($H_v$).

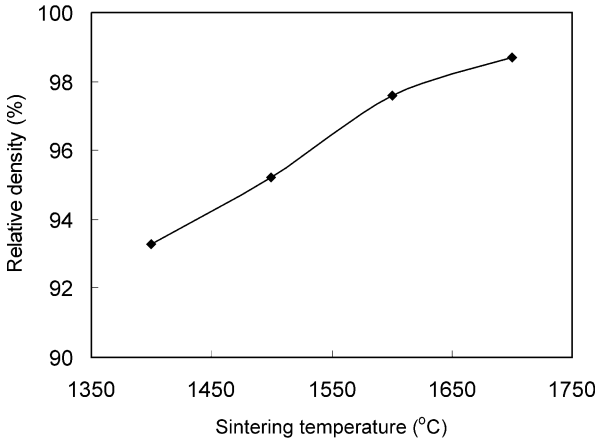


Fig. 7. Relationship between density of $MoSi_2$–20 wt.% TiC with 1 wt.% carbon and sintering temperature.

composites. The relative density decreases from 98.5% for $MoSi_2$–20 wt.% TiC to 97.6% for $MoSi_2$–20 wt.% TiC–1 wt.% C sintered at 1600 °C. The reduction in density decrease with increasing carbon content may explain the hardness decrease.

### 3.2.2. Sintering temperature effect on the mechanical properties of $MoSi_2$–20 wt.% TiC–1 wt.% C

Fig. 6 shows the mechanical properties of $MoSi_2$–20 wt.% TiC–1 wt.% C composite sintered at different temperatures. The results indicate that the bending strength of the composite strongly depends on the sintering temperature. The bending strength and fracture toughness increase then decrease with increasing temperature and reach their maxima of, respectively, 689 MPa and 5.4 $MPa{\cdot}m^{1/2}$ at 1600 °C. The relative density of $MoSi_2$–20 wt.% TiC–1 wt.% C increases with the sintering temperature as shown in Fig. 7, reaching 98.7% at 1700 °C. A high temperature is helpful for densification because the $MoSi_2$ matrix does not react with TiC at the sintering temperature. The increase of bending strength and fracture toughness between 1400 and 1600 °C is an effect of improved densification. The decay of such properties observed beyond 1600 °C can be attributed to grain growth, which modifies the mode of fracture propagation. While fully intergranular fracture has been reported [19] in case of fine-grained monolithic $MoSi_2$, a mixed-mode of transgranular and intergranular fracture occures in the coarse-grained $MoSi_2$/SiC composite and the rate of transgranular will increase with increasing grain size. Intergranular fracture, which has a long crack path in fine-grained composites will consume more energy than transgranular fracture in crack propagation, so improving the mechanical properties of composites.

According to the theory of particle-reinforced ceramics [20], the contribution of particles to the mechanical properties are (1) crack deflection which is based on the geometrical progress of a crack that has been deflected from its main crack plane, and (2) the residual stress caused by the thermal mismatch between the matrix and the reinforcement particles. For the $MoSi_2$–TiC composite, the thermal expansion coefficients of the $MoSi_2$ matrix and TiC particles are, respectively, $\alpha_m = 8\times10^{-6}$ m $K^{-1}$ and $\alpha_P = 7.4\times10^{-6}$ m $K^{-1}$ and the thermal mismatch is

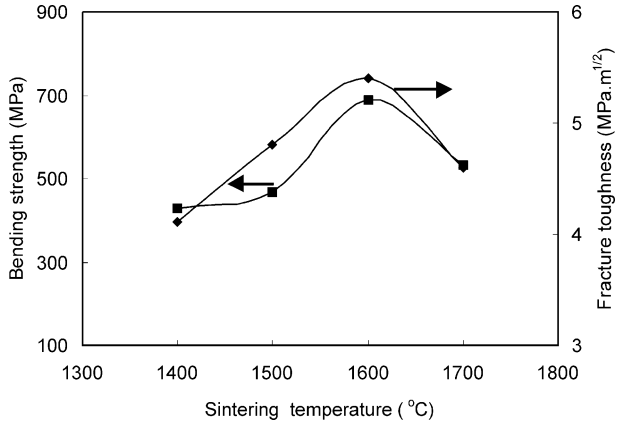


Fig. 6. Mechanical properties of $MoSi_2$–20 wt.% TiC with 1 wt.% carbon additive at different temperatures.

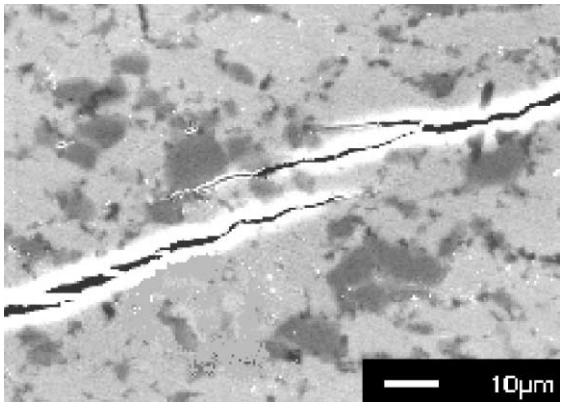


Fig. 8. Crack propagation SEM micrograph of $MoSi_2$–TiC–1 wt.% C composite (1600 °C).

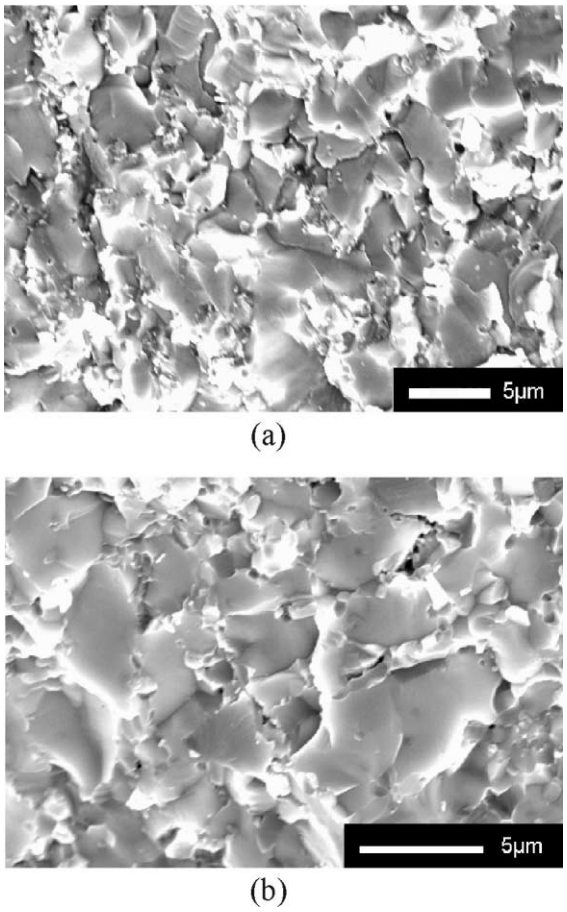


Fig. 9. Fracture surface SEM micrographs of (a) $MoSi_2$–20 wt.% TiC and (b) $MoSi_2$–20 wt.% TiC–1 wt.% C (1600 °C).

not, accordingly, very important. Therefore, the effectiveness of the TiC reinforcement is expected to consist mainly in crack deflection. Fig. 8 shows a SEM micrograph of a crack propagating through $MoSi_2$–TiC–1 wt.% C. After carbon is added to the composite, the glassy $SiO_2$ phase at the grain boundaries changes into in-situ SiC due to the chemical reactions between the $SiO_2$ and carbon, and modifies the combing strength among grains and the residual stress across the interfaces. As shown in the micrograph, the crack is significantly deflected and there is evidence also of bridging and branching, which can absorb a large amount of energy to improve the mechanical properties of the composite. The fracture surface observed in SEM micrographs of $MoSi_2$–20 wt.% TiC and $MoSi_2$–20 wt.% TiC–1 wt.% C reveals in both materials a wavy fractography which indicates crack deflection. In Fig. 9a, the fracture surface of $MoSi_2$–20 wt.% TiC is not clean and there is evidence of amorphous materials which may be $SiO_2$ between the grain boundaries, whereas in Fig. 9b the grain boundaries are very clean. All such results can explain how carbon addition can influence the mode of crack propagation and the mechanical properties of $MoSi_2$–20 wt.% TiC composites.

## 4. Conclusion

As a deoxidant, carbon was added to the $MoSi_2$–20 wt.% TiC composite, the glassy $SiO_2$ phase in $MoSi_2$–20 wt.% TiC composite grain boundaries can be eliminated due to the chemical reactions between carbon and $SiO_2$. The results show that the mechanical properties of the $MoSi_2$–20 wt.% TiC composites with carbon addition can be significantly modified. Compared with the mechanical properties of $MoSi_2$–20 wt.% TiC composite sintered at 1600 °C, 25 MPa, the bending strength and fracture toughness of the $MoSi_2$–20 wt.% TiC–1 wt.% C can be raised from 481 to 689 MPa and 3.89 to 5.4 MPa $m^{1/2}$, respectively. However, the mechanical properties of $MoSi_2$–20 wt.% TiC are strongly dependent on tightly linked to the addition of carbon and sintering temperature. An excess of carbon is harmful to the mechanical properties.

## References

[1] J.M. Yang, W. Kai, S.M. Jeng, Scripta Metall. 23 (1989) 1953–1958.
[2] L. Zheng, Y. Jin, P. Li, Compos. Sci. Technol. 57 (4) (1997) 463–469.
[3] D. Yi, C. Li, $MoSi_2$–$ZrO_2$ composites-fabrication, microstructures and properties, Mater. Sci. Eng.: A 261 (1–2) (1999) 89–98.
[4] A. Newman, S. Sampath, H. Herman, Mater. Sci. Eng.: A 261 (1–2) (1999) 252–260.
[5] J. Pan, M.K. Surappa, R.A. Saravanan, B.W. Liu, D.M. Yang, Mater. Sci. Eng.: A 244 (2) (1998) 191–198.
[6] A.M. Baker, P.S. Grant, R.G. Castro, H. Kung, Mater. Sci. Eng.: A 261 (1–2) (1999) 196–203.
[7] M.G. Hebsur, Mater. Sci. and Eng.: A 261 (1–2) (1999) 24–37.
[8] Hojo, Y. Ishizka, K. Kishi, S. Umebayashi, J. Jpn. Soc. Powder and Powder Metall. 42 (11) (1995) 1295–1299.
[9] S.A. Maloy, J.J. Lewandowski, A.H. Heuer, J. Petrovic, J. Mater. Sci. Eng. A155 (159-163).
[10] A. Costa e Silva, M.J. Haufman, Scripta Metall. Mater. 29 (8) (1993) 1141–1145.
[11] Y. Suzuki, P.E.D. Morgan, K. Niihara, J. Am. Ceram. Soc. 81 (12) (1998) 3141–3149.
[12] A.K. Vasudevan, J.J. Petrovic, Mater. Sci. Eng. A155 (1995) 1.
[13] P.J. Meschter, D.S. Schwartz, JOM 41 (1989) 52.
[14] R. Gibala, A.K. Ghosh, D.C. Vanaken, D.J. Srolovitz, A. Basu, H. Chang, D.P. Mason, W. Yang, Mater. Sci. Eng. A155 (1992) 147.
[15] S. Maloy, A.H. Heuer, J. Lewandowski, J. Petrovic, J. Am. Ceram. Soc. 74 (10) (1991) 2704–2706.
[16] W.A. Maxwell, Proceeding of the Metallurgy and Material Information Meeting, Vol. 1, Report No TID-5061, Journal Announcement; NSA 12, 1951.
[17] I. Pho, H.W. King, S. Das Gupta, J Canadian Ceram. Soc. 66 (1) (1997) 56–63.
[18] K. Niihara, R. Morena, D.P.H. Hasselman, J. Mater. Sci. Lett. 1 (1) (1982) 13–16.
[19] R. Mitra, Y.R. Mahajan, N.E. Prasad, W.A. Chiou, Mater. Sci. and Eng. A225 (1997) 105–117.
[20] K.T. Faber, A.G. Evans, Crack deflection process—I, Theory, Acta Metall. 31 (1983) 565–576.